Journal of Physics: Conference Series **267** (2011) 012012 doi:10.1088/1742-6596/267/1/012012

Structure effects in the reactions ^{9,10,11}Be+^{64}Zn at the Coulomb barrier

V Scuderi[1,2,3], A Di Pietro[2], L Acosta[4], F Amorini[1,2], M J G.Borge[5], P Figuera[2], M Fisichella[1,2], L M Fraile[6†], J Gomez-Camacho[7], H Jeppesen[6§], M Lattuada[1,2], I Martel[4], M Milin[8], A Musumarra[2,9], M Papa[2], M G Pellegriti[1,2], F Perez-Bernal[4], R Raabe[10],G Randisi[1,2‡], F Rizzo[1,2], D Santonocito[2], G Scalia[1,2], O Tengblad[5], D Torresi[1,2], A M Vidal[5], M Zadro[11]

[1]Dipartimento di Fisica ed Astronomia Università di Catania, Catania, Italy
[2]INFN-Laboratori Nazionali del Sud and Sezione di Catania, Italy
[3]Centro Siciliano di Fisica Nucleare e Struttura della Materia, Catania, Italy
[4]Departamento de Fisica Aplicada Universidad de Huelva, Huelva, Spain
[5]Instituto de Estructura de la Materia CSIC, Madrid, Spain
[6]CERN, Geneva, Switzerland
[7]Departamento de Fisica Atomica Molecular Nuclear Universidad de Sevilla, Sevilla, Spain
[8]Department of Physics Faculty of Science University of Zagreb, Zagreb, Croatia
[9]Dipartimento di Metodologie Fisiche e Chimiche per l'Ingegneria Università di Catania,Catania, Italy
[110]Instituut voor Kern-en Stralingsfysica University of Leuven, Leuven, Belgium
[11]Division of Experimental Physics Ruder Bo·skovic Institute, Zagreb, Croatia

E-mail: scuderiv@lns.infn.it

Abstract. Elastic scattering and direct reactions have been studied for the collisions induced by the three Beryllium isotopes ^{9,10,11}Be, on a medium mass ^{64}Zn target at energies around the Coulomb barrier. The elastic scattering angular distributions, measured for the three systems at the same center of mass energy, were analyzed within the Optical Model and reaction cross-sections were deduced from optical model calculations. For the ^{11}Be induced reaction the transfer/break-up angular distribution was also extracted.

1. Introduction

In the last years scattering of halo nuclei has been studied to some extent in the attempt to investigate both the influence of the projectile halo structure and low binding energy and the effect of the break-up coupling on the reaction dynamics. Since elastic-scattering is a peripheral process it probes the tail of the wave function and hence one can learn about surface properties, such as size of nuclei and surface diffuseness. Therefore, elastic-scattering is an ideal tool to study peculiar nuclear structures as for example the nuclear halo. As it is well known, the nuclear halo structure originates when very

†present address: Departamento de Fisica Atomica, Molecular y Nuclear, Universidad Complutense, Madrid, Spain
§present address: Nuclear Science Division, Lawrence Berkeley National Laboratory, Berkeley, USA
‡present address: LPC-ENSICAEN, IN2P3-CNRS and Universitè de Caen, France

weakly bound valence nucleon(s) can tunnel into the classically forbidden region, giving rise to a diffuse tail surrounding a well bound core. The weakly bound halo structure may affect also the reaction mechanisms in collisions induced by such nuclei especially at energies around the Coulomb barrier where couplings between the entrance channel and the continuum [1-5], as well as to the various reaction channels [6-9] are expected to be very important. Direct reactions, such as break-up or transfer, may be favored owing to the low binding energy, the extended tail of halo nuclei and the large Q-values for selected transfer channels.

From an experimental point of view, high quality data are necessary; however, due to the low intensities of the radioactive beams, these are not always available. Since ^{6}He beams are available in different facilities with intensities up to 10^{7} pps, in a wide range of energies, several experiments have been performed so far using mainly this two neutron halo nucleus on different targets. A common feature, observed in the ^{6}He induced elastic scattering, is a reduction of the cross-section in most of the measured angular range [10,11]. As a consequence of the elastic cross-section suppression, the total reaction (TR) cross-section is found to be much larger, a factor of 2 in some cases, than the one observed in reactions induced by non-halo nuclei [10,12].

Optical Model (OM) calculations [11-13] have shown that the optical potential of halo and weakly bound nuclei has a long range part due to the coupling to non-elastic channels and that a large diffuseness parameter of the imaginary potential is needed in order to take into account the diffuse structure of the ^{6}He halo and to describe the data. Continuum Discretized Coupled Channel calculations (CDCC) of the ^{6}He elastic scattering on different target masses (e.g. [2-4]) have been recently published. According to these calculations, the suppression of the elastic cross-section at forward angles is mostly originated by the coupling to states into the continuum. Besides coupling to bound and unbound states, also coupling to one and two neutron stripping can be of importance in describing the low-energy scattering of a halo nucleus. This has been investigated in (e.g. [6-7]) and according to the authors it has a significant effect on the elastic scattering of ^{6}He and should not be neglected. Moreover, coupling effects of break-up or transfer depend upon nuclear structure properties of projectile and/or target as well as break-up thresholds or beam energies. Therefore drawing general conclusions about channel coupling effects on a limited sets of reactions induced by ^{6}He could be misleading. Moreover, due to the complexity of modelling reactions with the 2n-halo ^{6}He it would be of great help to have detailed elastic scattering data of 1n-halo systems, such as ^{11}Be.

To our knowledge, only two attempts to measure elastic-scattering and reaction mechanisms around the barrier with n-halo nuclei different than ^{6}He are reported in literature. ^{11}Be+^{209}Bi was measured by Mazzocco *et al.* [15-16], using a fragmentation beam degraded in energy. The quasi elastic cross-section, which included inelastic excitations up to 2.6 MeV, was measured. The extracted TR cross-section was found to be similar to the one of ^{9}Be+^{209}Bi, measured by the same group [17]. The authors concluded that the breakup process has comparable strengths in both ^{9,11}Be nuclei and that the differences in binding energies and radii of the two Be isotopes do not play an important role. This result is not in agreement with what observed by different authors in ^{6}He induced collisions. In [18] ^{11}Be+^{120}Sn quasi-elastic-scattering angular distribution was measured, the ^{11}Be(1/2-) inelastic excitation was included, but in a very limited angular range.

Recently, we have measured the elastic scattering angular distributions for the collisions induced by the three different Be isotopes, ^{9,10,11}Be, on a medium mass ^{64}Zn target in a wide angular range and with small angular step at $E_{c.m.}$= 24.5 MeV, close to the coulomb barrier [19]. By comparing the elastic-scattering angular distributions for these three systems, the separate effect of the weak binding and halo structure can be investigated. Moreover, in the case of the halo ^{11}Be nucleus the transfer/break-up cross-section has been measured, as well.

2. Experimental Set-up

The experiment with the stable ^{9}Be beam was performed at Laboratori Nazionali del Sud (LNS) in Catania. The ^{9}Be beam was delivered by the SMP 14MV Tandem of LNS and was impinging on a 550 μm/cm^{2} ^{64}Zn. The light charged particles, emitted in the reaction, have been detected using five ΔE (~

10 μm thick) - E (~ 150 μm thick) Si detector telescopes each consisting of a surface barrier detector. The five telescopes were placed on a rotating arm allowing the measurement of the elastic scattering angular distribution up to 110°.

The data with the radioactive beams were obtained, in the same experiment, using the new post accelerated ^{10,11}Be beams of REX-ISOLDE at CERN. The detection system, shown in fig. 1, consisted of 6 ΔE (~ 50 μm thick) - E (~ 1500 μm thick) Si detector telescopes, each one with a surface of 50x50mm^2, surrounding a thin ^{64}Zn target (550 μg/cm^2 and 1000 μg/cm^2 for the ^{10,11}Be beams, respectively). The target was tilted at 45° to allow the measurement in the angular region around 90°. The ΔE stage consists of a Double sided Silicon Strip Detector (DsSSD) segmented in 16 both on the front side and on the rear side, allowing a 256 pixels for each detector. The E stage consists of a Silicon Single Pad detector. The detectors were placed very close to the target in order to have a large polar angle (10°<θ<150°) and solidangle coverage. The average beam intensity was 10^6 pps and 10^4 pps for ^{10}Be and ^{11}Be, respectively.

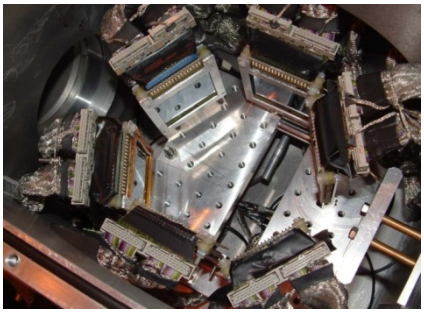

Figure 1. Picture of the detectors set-up inside the scattering chamber

The effective solid angles covered by each detector pixel have been evaluated by using a Monte Carlo simulation code. However, due to the very compact geometry of the detection system, small variations of the beam position onto the target resulted in a large variation of the detector angles. Therefore, polar angle and solid angle determination has been verified by measuring the Rutherford scattering for the ^{12}C+^{197}Au reaction at E_{lab} = 28 MeV as well as the elastic scattering angular distribution for the collision ^{10}Be+^{197}Au at E_{lab} = 29.4 MeV. With the adopted analysis procedure, the expected Rutherford behaviour of the cross-sections for the two reactions were obtained, indicating that the geometry was properly determined.

3. Results and Discussion

In Fig. 2 the angular distributions for the scattering of ^{9,10,11}Be+^{64}Zn are shown in linear scale. We must say that, as in [15], also in the present case the ^{11}Be+^{64}Zn scattering cross-section is the quasi elastic cross-section, since the inelastic contribution of the *1*st excited state of ^{11}Be at E_x=320 keV is included. However, the possible contribution to the scattering cross-section of the inelastic channel has been evaluated by performing OM calculations using as dipole strength B(*E*1)=0.115e^{2}fm^2 [20] and the potential parameters extracted from the fit of the scattering data. According to the these calculations (see ref. [19]), the inelastic contribution to the scattering cross-section is quite small at all measured angles and therefore negligible. For this reason we refer to the angular distribution for ^{11}Be+^{64}Zn as elastic scattering angular distribution.

As one can see from fig. 2, in spite of the very different binding energies of ^{9}Be and ^{10}Be, their elastic-scattering angular distributions are similar. On the contrary, as one can see in fig. 2, ^{11}Be scattering shows a very different pattern and the main feature that one can observe is a strong reduction of the elastic cross-section at forward angles. In [1] the suppression of the scattering cross-section at small angles, in collision induced by weakly bound nuclei, is connected to the coupling with

a large Coulomb dipole due to the presence of the low-lying electric dipole strength. The authors studied also the dependence of the suppression of the cross-section from the target charge and beam energy concluding that this effect, close to the Coulomb barrier, should be evident only in scattering with targets having high charge (Z_T ~80) and that measurements with lighter targets (Z_T ~28) are not sensitive to this coupling. This would explain the similar angular distribution for ^{9,10}Be scattering. Indeed, in the ^{6}He induced collisions, a clear reduction of elastic cross-section at small angles has been observed although not as large as in the present case and only for heavy targets [11]. The elastic scattering angular distribution of ^{6}He on a medium mass target ^{64}Zn does not show such feature [10]. Thus, the observation of a strong reduction of elastic cross-section at small angles in the scattering of ^{11}Be which has a strong low-lying continuum dipole strength, as ^{6}He and ^{9}Be, with a light charge target must be due to other mechanisms besides coupling to Coulomb break-up, that could be associated with the halo structure.

The observed difference in ^{6}He and ^{11}Be scattering could be due to the more extended halo distribution in ^{11}Be compared to ^{6}He (e.g. [21]).

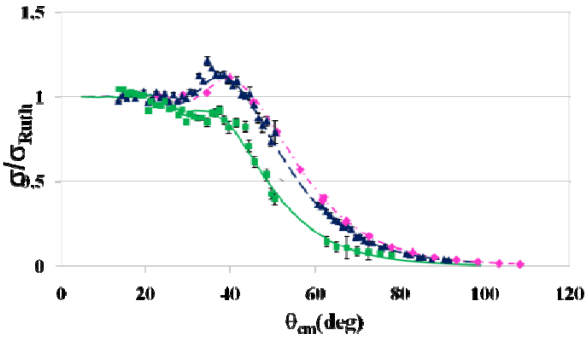

Figure 2. Elastic-scattering angular distributions on ^{64}Zn: ^{9}Be(diamonds), ^{10}Be (triangles) and ^{11}Be (squares). The lines represent the OM calculations for ^{9}Be(dot dashed), ^{10}Be (dashed) and ^{11}Be (full line).

The ^{9,10,11}Be+^{64}Zn elastic-scattering data were analyzed within the OM framework using the code PTOLEMY [22]. For ^{9,10}Be a Woods-Saxon (W-S) form of the real and imaginary potential was used. In the case of ^{11}Be, in order to take into account the diffuse halo structure and the effect of the break-up channel on elastic scattering, a surface term was added to the imaginary volume potential.

Couplings can be represented in the OM by the addition of a complex dynamic polarization potential (DPP) to the OP (e.g. [23]). In [24] the DPP was a surface potential calculated analytically and applied to the ^{11}Be+^{12}C data at 49.3 AMeV. The real part of the DPP was not considered in the calculations since it produced a negligible effect on the elastic scattering fit. The volume potential, responsible for the inelastic core-target interaction, was obtained from the fit of the scattering of the ^{10}Be core on the same target. The calculated surface potential was responsible for peripheral reactions like transfer or break-up. This term has an exponential tail, and a diffuseness parameter of 3.2 fm. A similar result was also obtained in [21]. Then, we used a procedure similar to [24] to deduce the optical potential in the case of ^{11}Be+ ^{64}Zn.

In the present case, all terms of the OP were extracted phenomenologically from a fit of the elastic scattering angular distributions. The fit of ^{11}Be+^{64}Zn was performed using as volume part of the real and imaginary W-S potentials the ones obtained from the fit of the scattering data of the core ^{10}Be on ^{64}Zn and in addition we considered a surface imaginary term having the shape of a W-S derivative. The effect of such term, as one can see from fig. 2, is to reduce the scattering cross-section at all the measured angles and in particular in order to reproduce the behaviour of the cross-section at forward angles we have found that a very large surface diffuseness parameter is needed, a_{si}= 3.5 fm. The surface diffuseness and also the surface potential depth, extracted from the fit, are consistent with [24].

The large diffuseness confirms the presence of long range absorption mechanisms. The suppression of the elastic cross-section at forward angles is then originated by absorption occurring at large impact parameters due to the diffuse halo structure of the ^{11}Be. More details on the OM analysis and the potential parameters are reported in [19].

From the OM analysis we have also extracted TR cross-section for all the reaction studied. The deduced TR cross-sections are $\sigma_{TR} \sim 1$ b for ^{9}Be, $\sigma_{TR} \sim 1.2$ b for ^{10}Be and $\sigma_{TR} \sim 2.7$ b for ^{11}Be. Consequently to the reduction of the elastic cross-section, we have observed a much larger TR cross-section in the halo ^{11}Be nucleus case with respect the other two Be isotopes.

Since the TR cross-section for the ^{11}Be case is double than the one for the ^{9,10}Be cases, it is important to understand if such enhancement could be due to transfer and/or break-up processes as observed in the ^{6}He case [10,25,7]. Indeed, when comparing the ΔEvsE spectra for the reactions induced by ^{10}Be and ^{11}Be, shown in fig. 3, events close to the elastic and consistent with the detection of ^{10}Be coming from transfer and/or break-up processes are present in the ^{11}Be beam case. On the contrary, similar events are not observed in the ^{10}Be case. In fig. 4 the angular distribution for such events is shown. The corresponding integrated cross-section is $\sigma = 1100 \pm 150$ mb. This cross-section corresponds to about 40% of the TR cross-section measured for ^{11}Be. This result confirms what was found in the ^{6}He experiments (e.g. [10, 12]) but disagrees with the previously published data of ^{11}Be [15,16].

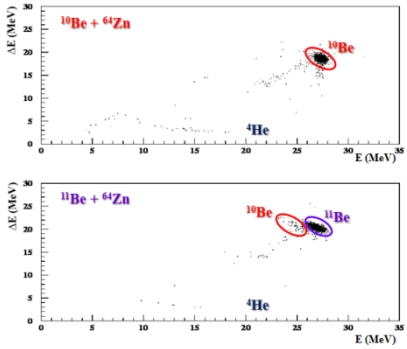

Figure 3. Δ*E*vs*E* scatter plots for the reactions ^{10}Be+^{64}Zn (top) and ^{11}Be+^{64}Zn (bottom), at θ=35°

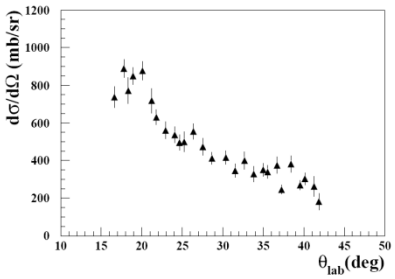

Figure 4. Angular distribution of transfer/break-up events in ^{11}Be+^{64}Zn obtained by selecting ^{10}Be events in the Δ*E*vs*E* spectrum.

4. Couclusion

In summary, we have studied the collisions ^{9,10,11}Be+^{64}Zn at energy close to the Coulomb barrier using high quality post-accelerated beams. The scattering of the ^{11}Be halo nucleus shows extremely different

features with respect the ^{9}Be and ^{10}Be. The ^{11}Be elastic cross-section is strongly suppressed and absorption occurs at much smaller scattering angles than for the other two Be isotopes.

All the scattering data were interpreted within the OM. In order to take into account the ^{11}Be diffuse halo structure and to reproduce the scattering data a surface imaginary potential with a very large diffuseness parameter was needed. Along with the OM parameters the TR cross-section were also deduced and we have found that in the ^{11}Be halo nucleus case the TR cross-section is much larger than the ones for ^{9,10}Be induced reaction.

Moreover, from the analysis of ^{10}Be events, present in the collision induced by the ^{11}Be halo nucleus, it was found that about 40% of the TR cross-section can be attributed to transfer and/or break-up processes.

These results show a strong effect on nuclear reaction mechanisms around the barrier due to the ^{11}Be halo structure and to its weak binding and represents an independent confirmation that similar effects observed for the ^{6}He are also due to its halo nature.

References

[1] Kucuk Y et al., 2009 *Phys. Rev.* C 79, 067601.
[2] Moro A et al., 2007 *Phys. Rev.* C 75, 064607.
[3] Matsumoto T et al., 2006 *Phys. Rev.* C 73, 051602R.
[4] Rodriguez-Gallardo M et al., 2008 *Phys. Rev.* C 77, 064609.
[5] Rusek K et al., 2005 *Phys. Rev.* C 72, 037603.
[6] Keeley N and Alamanos N, 2008 *Phys. Rev*. C 77, 054602.
[7] Chatterjee A et al., 2008 *Phys. Rev. Lett.* 101, 032701.
[8] Keeley N et al., 2009 *Prog. Part. Nuc. Phys.* 63, 396.
[9] Keeley N et al., 2007 *Prog. Part. Nuc. Phys*. 59, 579.
[10] Di Pietro A et al., 2004 *Phys. Rev.* C 69, 044613.
[11] Sanchez-Benitez A M et al., 2008 *Nucl. Phys.* A 803, 30.
[12] Aguilera E et al., 2001 *Phys. Rev.* C 63, 061603(R).
[13] Kakuee O et al., 2003 *Nucl. Phys.* A 728, 339.
[14] Moro A et al., 2007 *Phys. Rev*. C 75, 064607.
[15] Mazzocco M et al., 2006 *Eur. Phys. J*. A 28, 295.
[16] Mazzocco M et al., 2007 *Eur. Phys. J*. S. T. 150, 37.
[17] Signorini C et al., 2002 *Nucl. Phys.* A 701, 23c.
[18] Acosta L et al., 2009 *Eur. Phys. J* A 42, 461.
[19] Di Pietro A et al., 2010 *Phys. Rev. Lett.* 105, 022701.
[21] Hassan M et al., 2009 *Phys. Rev.* C 79, 064608.
[22] Rhoades-Brown M et al., 1980 *Phys. Rev*. C 21, 2417.
[23] Satchler G, 1991 *Phys. Rep.* 199, 147.
[24] Bonaccorso A and Carstoiu F, 2002 *Nucl. Phys. A* 706, 322.
[25] Young P D et al., 2005 *Phys. Rev.* C 71, 051601R.